



**HAL**  
open science

# Towards local bioeconomy: A stepwise framework for high-resolution spatial quantification of forestry residues

S.K. Karan, L. Hamelin

## ► To cite this version:

S.K. Karan, L. Hamelin. Towards local bioeconomy: A stepwise framework for high-resolution spatial quantification of forestry residues. *Renewable and Sustainable Energy Reviews*, 2020, 134, pp.110350. 10.1016/j.rser.2020.110350 . hal-03006625

**HAL Id: hal-03006625**

**<https://hal.inrae.fr/hal-03006625>**

Submitted on 21 Sep 2022

**HAL** is a multi-disciplinary open access archive for the deposit and dissemination of scientific research documents, whether they are published or not. The documents may come from teaching and research institutions in France or abroad, or from public or private research centers.

L'archive ouverte pluridisciplinaire **HAL**, est destinée au dépôt et à la diffusion de documents scientifiques de niveau recherche, publiés ou non, émanant des établissements d'enseignement et de recherche français ou étrangers, des laboratoires publics ou privés.



Distributed under a Creative Commons Attribution - NonCommercial 4.0 International License

## Towards local bioeconomy: A stepwise framework for high-resolution spatial quantification of forestry residues

Karan, S.K.<sup>1,\*</sup> and Hamelin, L.<sup>1</sup>

1. Toulouse Biotechnology Institute (TBI), INSA, INRAE UMR792 and CNRS UMR5504, Federal University of Toulouse, 135 Avenue de Rangueil, F-31077, Toulouse, France

\* Corresponding Author:

Email: [karan@insa-toulouse.fr](mailto:karan@insa-toulouse.fr), Tel.: +33 051-155-9791

### Abstract:

In the ambition of a transition from fossil carbon use, forestry residues are attracting considerable attention as a feedstock for the future bioeconomy. However, there is a limited spatially-explicit understanding of their availability. In the present study, this gap has been bridged by developing a generic framework “CamBEE”, for a transparent estimation of aboveground primary forestry residues. CamBEE further includes guidelines, based on standard uncertainty propagation techniques, to quantify the uncertainty of the generated estimates. CamBEE is a four-step procedure relying on open-access spatial data. The framework further provides insights on the appropriate spatial resolution to select. In this study, the proposed framework has been detailed and exemplified through a case study for France. In the case study, primary forestry residues have been spatially quantified at a resolution of 10 m, using spatial and statistical data on forest parameters (net annual increment, factor of basic wood density, biomass expansion factors, etc.). The results for the case study indicate a total theoretical potential of 8.4 Million Mg<sub>dry matter</sub> year<sup>-1</sup> (4.4 – 13.9 Million Mg<sub>dry matter</sub> year<sup>-1</sup>) available in France, the equivalent of 161 PJ year<sup>-1</sup>. The case study validates that the CamBEE framework can be used for high-resolution spatial quantification of PFRs towards integration in local bioeconomy.

### Highlights:

- CamBEE: A framework for high-resolution spatial quantification of forestry residues
- Uses open-source spatial data & presents results with uncertainties
- A metric for deciding the spatial resolution for such assessments is provided
- Exemplified results for France reveal 8.4 Million t DM y<sup>-1</sup> of forestry residues

**Keywords:** *Bioeconomy; Forest Residues; Fossil carbon transition; Spatial Quantification; Theoretical Potential; Uncertainty Assessment.*

**Word Count:** 8008

### List of Abbreviations

°C	Degree Celsius
ALS	Airborne Laser Scanning
BEE	Biomass Energy Europe
BEF	Biomass Expansion Factor
CCI	Climate Change Initiative
CLC	CORINE land cover
D	Factor of basic wood density
d.b.h.	Diameter at breast height
EU	European Union
FA	Forest Area
FAO	Food and Agriculture Organization
FRAs	Forest Resource Assessments
GAI	Gross Annual Increment
GIS	Geographic Information System

GLS	Global Land Survey
GRECO	<i>Grandes Régions Écologiques</i>
GUM	Guide to Uncertainty in Measurement
IPCC	Intergovernmental Panel on Climate Change
MODIS	Moderate Resolution Imaging Spectroradiometer
Mg <sub>dry matter</sub> year <sup>-1</sup>	Megagram (1 tonne) of dry matter per year
NAI	Net Annual Increment
NFIs	National Forest Inventories
NL	Natural Losses
NPP	Net Primary Productivity
PFRs	Primary Forestry Residues
PJ year <sup>-1</sup>	Petajoule per year
SER	<i>Sylvoécorégions</i>

## 1. Introduction

Facing the emergency to limit the global mean temperature to 1.5°C above pre-industrial levels [1], additional releases of fossil carbon must be prevented, while sinks must be induced to achieve so-called carbon neutrality [2,3]. By using biogenic carbon to supply materials, chemicals, food, and energy services, bioeconomy is one option to reach the balance between anthropogenic emissions and sinks. In particular, the use of biomass residues has generated growing interest as a feedstock not associated with land-use changes [4–6], Hamelin et al. [4] highlighted a total (or theoretical) residual biomass potential of 8500 PJ year<sup>-1</sup> for EU-27 + Switzerland, with forestry residues representing ca. 37% of this potential.

Forestry residues can be divided into two categories [8]; (i) Primary forestry residues (PFRs), and (ii) Secondary forestry residues. PFRs are defined as residues that are left after logging operations (branches, stumps, treetops, bark, sawdust, etc.). In contrast to PFRs, secondary forestry residues are by-products and co-products of industrial wood-processing operations (bark, sawmill slabs, sawdust, wood chips, etc.). This study focuses solely on aboveground PFRs (Figure 1). Accordingly, belowground stumps and roots are excluded, given the heavy concerns related to the environmental [9,10] and economic sustainability of harvesting these [11].

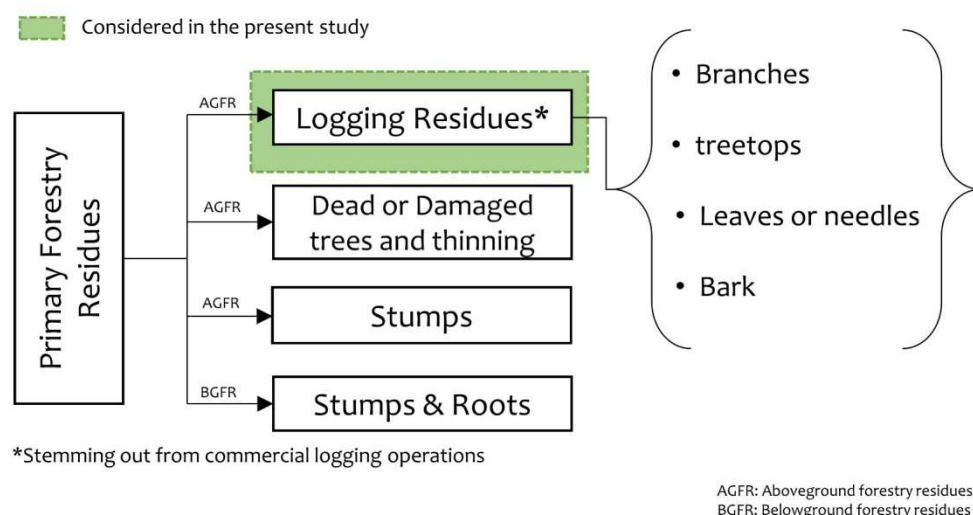


Figure 1: Primary forestry residues (PFR) and streams considered in this study

When it comes to spatial quantification of PFRs, the methods have generally improved over the last ten years, but due to a lack of standardization, there is still a significant concern in the user community on the available methods and practices [12,13]. Spatial quantification of PFRs is here defined as quantifying the amount of PFR generated per unit area along with positional attributes (Supplementary Table 1). Besides the lack of

standardization on methods and definitions, the availability of spatially-explicit forest data on forest classes, species, annual increment, expansion factors, etc. is a major limiting factor for such assessments. This is especially true for regions with diverse physiography [14]. One well-known forest data inventory is FAO's "Forest Resource Assessments" (FRAs) [15], which provides spatial data on forest statistics. Although valuable, the spatial data provided by FRAs are at best at the country scale, hence unsuitable for high-resolution mapping for use in developing local deployment strategies. The data countries supply to the FAO for the FRA typically stem from National Forest Inventories (NFIs), which provide comprehensive data on forestry [16] at sub-regional, regional, or country scales. Despite major harmonization efforts, the aggregation of these national data in FRA reports still present severe discrepancies regarding nomenclature, baseline variables, etc. [17–19]. For example, the Swiss NFI only measures trees with the diameter at breast height (d.b.h.)  $\geq 12$  cm for quantifying growing stock [20]. In contrast, this threshold is 0 cm (hence including the complete stem top) in the reference definition of Cost Action E43 [21], a landmark in Europe for harmonized NFI definitions [17].

Furthermore, one vital consideration for spatial quantification is the scale and spatial resolution that is being used. For geographic information system (GIS) applications, it is a common practice to merge datasets through the use of different functions, such as map overlay. But if datasets do not have harmonized spatial resolutions, the result of this operation becomes erroneous. In simple words, spatial scale refers to the size of a land area or geographic distance studied. However, there are various categories of scale, such as geographic, operational, measurement, and cartographic, and it is essential that a clear distinction is made amongst them. The definition of these terminologies is provided in Supplementary Table 1. Most studies on spatial quantification do not consider spatial scale as an important parameter; instead, in general, the studies directly use certain spatial data related to the available methods without questioning the uncertainties associated with them. For example, the use of local forest inventory statistics on a global or continental assessment would lead to a large amount of uncertainty in the analysis due to inconsistencies in geometry, attributes, and semantics owing to scale differences [22]. In fact, when it comes to high-resolution mapping of residual biomass resources at country scales, there is no real discussion on what resolution can be considered as useful for bioeconomic purposes.

Globally, very few studies have attempted to spatially quantify the potential of residual biomass from forestry and none of them report the uncertainty associated with the results. A brief critical summary of some of these studies is presented in Table 1.

[Table 1 here]

Table 1: Critical summary of studies on spatial quantification of Primary Forestry Residues, in chronological order

Ref*	Brief detail about the method	Scale / Year†	Data Used	Discussion
[23]	Based on a mathematical model using regression parameters and site-specific input data, including restriction parameters (e.g. slope, etc.).	Regional (**specify**) (Spain) / 2009	<ol style="list-style-type: none"> <li>1. The normal diameter of particular tree species.</li> <li>2. Annual increment in diameter of particular tree species, for the area of interest.</li> <li>3. Lower heating value.</li> <li>4. Site-specific parameters (Road map, slope map).</li> </ol>	<ul style="list-style-type: none"> <li>• The restriction parameters are highly subjective and lack standards.</li> <li>• It only considers “usable areas”.</li> <li>• Incorporates site-specific parameters (for technical and economic reasons).</li> <li>• Uses restriction modeling to estimate the technical potential.</li> <li>• Appropriate for a theme-based study (e.g. identification of suitable sites to supply a given thermal power plant).</li> <li>• Requires annual measurements of diameter increments.</li> </ul>
[24]	Based on ancillary data from literature coupled with GIS soil data and biomass growth rates.	Sub-regional (Mozambique) / 2009	<ol style="list-style-type: none"> <li>1. Forest growth data from the literature.</li> <li>2. Thematic cartography of soils.</li> <li>3. Forest productivity estimation using models from the literature.</li> <li>4. Land-cover map from Landsat data.</li> </ol>	<ul style="list-style-type: none"> <li>• Heavily reliant on data from the literature.</li> <li>• It does not use any site-specific forestry data.</li> <li>• Uses arbitrary modeling data from different African regions for simulating results.</li> <li>• Unclear methodology concerning the estimation of the PFRs, impossible to replicate.</li> </ul>
[25]	Based on allometric equations and site-specific forestry data for the evaluation of PFRs for different tree species.	Country (Portugal) / 2010	<ol style="list-style-type: none"> <li>1. Statistical data for diameter at breast height (d.b.h.) from field inventory.</li> <li>2. The total height of the trees from field inventory.</li> <li>3. Statistical data on forestry from literature.</li> </ol>	<ul style="list-style-type: none"> <li>• Almost totally estimated using statistical and allometric equations.</li> <li>• Fails to include a land cover or forest cover map for precise mapping (unless the spatially-explicit dataset is available for tree diameter and height). Fails to incorporate regions specific parameters.</li> <li>• Useful only for assessment involving different species.</li> <li>• Discretization at different scales not possible.</li> </ul>
[26]	Based on remote sensing, forest descriptive statistics and site-specific silvicultural model. Uses automated forest segmentation algorithm developed by Wells[27]	Regional/Sub-regional (USA) / 2016	<ol style="list-style-type: none"> <li>1. Remote sensing measurement (Aerial digital imagery)</li> <li>2. Stand characteristics, basal area, tree density, and above-ground biomass.</li> </ol>	<ul style="list-style-type: none"> <li>• Precise mapping even at sub-regional scale.</li> <li>• Very high spatial resolution.</li> <li>• Very high temporal resolution of 2 to 5 years.</li> <li>• Not replicable for use in different areas.</li> </ul>
[13]	A pixel-based approach that uses long-term forest inventory data in conjunction with remote sensing to generate logging residues availability map.	Country (Canada) / 2018	<ol style="list-style-type: none"> <li>1. Forest attribute maps which include above-ground biomass and percentage tree cover (250 m resolution)[28]</li> <li>2. Annual harvest maps (Specialized product called CanLaD[29])</li> </ol>	<ul style="list-style-type: none"> <li>• The method is a potential alternative to expensive field surveys.</li> <li>• It can be useful in predicting the amount of available logging residues in the future.</li> <li>• A complex approach that is not easily replicable and uses specialized processed products like annual harvest maps and forest attribute maps which might not be available for other regions.</li> </ul>
[4,30]	The approach used in these studies uses the forest raster data in conjunction with statistics on NAI and BEF, through a certain combination of logically defined equations. This method is further detailed in section 3.4.1 of [31] †	Continental (Europe)[4] / 2019  Regional (Emilia Romagna/Italy)[30] / 2019	<ol style="list-style-type: none"> <li>1. Raster/Vector data of forest area (ha)</li> <li>2. Raster/Vector data of average stemwood net annual increment per area based on inventory statistics (Region, Pixel, Raster) <math>m^3ha^{-1}year^{-1}</math></li> <li>3. Wood density for different forest type/species (<math>Mg_{dry\ matter\ m^{-3}}</math>)</li> <li>4. Biomass Expansion Factors</li> </ol>	<ul style="list-style-type: none"> <li>• Estimation involves multiple steps that can affect the accuracy of the estimated results.</li> <li>• Clear steps for the estimation of each parameter.</li> <li>• Can be used for assessment at various scales starting from plot to continental without compromising accuracy.</li> <li>• Involves using actual field data along with forest cover maps, thus, making it suitable for a variety of scales.</li> <li>• Explicitly described steps make incorporation of uncertainty possible.</li> </ul>
[32]	This approach uses national forest inventory data and relates it to several independent variables extracted from Airborne Laser Scanner (ALS) to create a model for quantification of forest residual biomass using a non-parametric regression approach.	Regional (Spain) / 2019	<ol style="list-style-type: none"> <li>1. Multi-Year field forest inventory</li> <li>2. ALS point cloud data</li> </ol>	<ul style="list-style-type: none"> <li>• Very high spatial resolution, ideal for sub-regional study.</li> <li>• Limited coverage (swath)</li> <li>• Only covers a particular specie (<i>Pinus halepensis</i>), hence it may not be suitable for complex forests with heterogeneous species.</li> </ul>

\* Ref: Reference of studies with spatial quantification of PFR; † The BEE best practices and methods handbook presents three methods for the estimation of stemwood and primary forestry residues viz.; basic spatially-explicit method, advanced spatially-explicit method, cost-supply method. Out of these three, only the first one allows for full transparency in terms of representing actual theoretical potential without any sustainability or feasibility constraints; ‡ Year of publication

As highlighted in Table 1, researchers have adopted several methods for estimating PFRs. The diversity of these methods is an indicator of the lack of standardization for such assessments. Furthermore, the approaches listed chronologically in Table 1 also emphasize how technological improvements in remote sensing have changed the data requirements over the years, with recent methods [13,26,32] relying on actual remote sensing measurements than purely being based on certain assumptions and models [23,24]. Despite this, almost all of the methods listed in Table 1 require field data from forest inventory or statistics for either initializing models or for validating the results. Field data are essential for robust estimation of PFRs, as the quantity of PFRs is primarily dependent on the harvesting practices, which varies spatially due to several factors such as forest type, harvesting policies, machinery, management practices, etc. Out of all the methods presented in Table 1, only those of [13] and [29] seem promising in the context of large geographic-scale high-resolution mapping. The other methods are either too conceptual, relying primarily on ancillary data from the literature [24], or would be unfeasible to implement for a country scale assessment due to expensive data and processing time [32].

The method developed in [13] is an approach to spatially estimate the quantity of logging residues by using remote sensing products. In their study, a set of multi-year harvest maps and a set of forest attribute maps along with inventory data from NFI were used, and finally, this data was aggregated per hectare of forest area. As reported by the researchers [13], the advantage of using this approach is to have an estimate on the future availability of the residues at a country scale. However, there are several constraints for the application of this method in different regions of the world such as, availability of long-term (decadal) harvest maps, availability for specialized products like “CanLaD” (a comprehensive dedicated regional database), etc., which limits the reproducibility of their approach in other regions. The shortcomings of this approach can be overcome by using the method provided by Vis and Van den Berg [31], also referred to as the BEE approach in this study. The BEE approach is the most transparent among all methods listed in Table 1, and amongst the only ones to describe the intermediate steps it uses, making it replicable and adaptable. Another advantage of using this technique is the use of both forest cover map and forest statistics in the intermediate steps of calculation. This eliminates the need for other assumptions, such as regression parameters [23] or allometric equations [25]. Consequently, the use of this method will likely better represent the actual ground condition with a lower degree of variability (depending on the quality of the input statistical data) compared to the other techniques listed in Table 1. Even with a constraint like limited availability of inventory statistics, this method can be used to estimate the quantity of PFRs based entirely on remote sensing data products (Forest cover map from CORINE Land Cover and Net Primary Productivity data from MODIS) with a certain degree of accuracy. Additionally, due to the discrete and flexible nature of the BEE approach, uncertainty accounting can easily be introduced in the intermediate steps of calculation. This would allow a significant improvement of the current method by generating final quantification results with a confidence interval. Ergo, the present study fully acknowledges and builds upon the efforts and knowledge developed within the BEE method.

From a theoretical viewpoint, spatial estimations are representations, and all representations of reality have their complexities that cannot be measured directly, which may be termed as potential error or uncertainty. For spatial assessments, uncertainty quantification not only gives a quantified idea about the confidence in calculated results (as ranges); it may also help to understand the spatial pattern of deviation, and ultimately lead to better decision making for the mobilization of the assessed resources. However, there is a severe dearth of studies incorporating uncertainty analysis in spatial quantification of forest residues; in fact, no literature reporting uncertainty in spatial quantification of forest residues has been found.

In an endeavor to bridge these gaps, this study aims to develop a replicable method for high-resolution spatial quantification of aboveground PFRs at the pixel level along with uncertainty quantification and to illustrate how to use it for a concrete case study. The study at hand also proposes a scheme for selecting the optimal resolution for the spatial quantification of PFRs based on several performance criteria. The methodology produced in this study intends to equip bioeconomy policymakers with reliable spatially-explicit estimates of this key stream for the future bioeconomy. Besides the investment decision itself, these high-resolution estimates could support decisions such as the siting of a bio-refinery unit.

The paper is structured as follows: Section 2 presents the scope of the study and defines the key terms used. Section 3 details the generic stepwise methodological framework proposed for high-resolution spatial

quantification of PFRs. Section 4 deals with the exemplification of the method. In section 5, the results of the study have been critically discussed, focusing mainly on the methodological framework and uncertainty associated with different data sources. The discussion section also includes a comparison of the results with other studies and how this work can be improved further. Based on these, the study concludes how the proposed methodology with uncertainty quantification is a definite step forward towards providing a transparent, replicable, and harmonized methodology for spatial quantification of PFRs.

## **2. Scoping**

An essential consideration in biomass resource assessment is the type of biomass potential being estimated. The BEE method [31], as well as several other studies, e.g., by Hamelin et al. [4], and Greggio et al [30], distinguish five types of biomass potentials, i.e., theoretical potential, technical potential, economic potential, implementation potential, and sustainable potential. The type of biomass potential being assessed largely determines the approach, methodology, and data requirement [31,33]. The theoretical potential is generally defined as the maximum overall amount of given targeted biomass that can be considered theoretically available, e.g., for bioeconomy. Other potentials, as per their labels, consider some restriction criteria to estimate the biomass resources. From the perspective of strategic decision making at the national level, the theoretical potential is viewed as the most suited, being the most transparent. The estimation of other potentials is usually associated with a certain degree of subjectivity and may apply constraints that could vanish with time, due to changing framework conditions. Hence, this study focuses only on evaluating the theoretical potential for PFRs.

The objective of this study is not to introduce new nomenclature, definition, or categorization. However, given the potential confusion related to the use of some key terms, the exact definitions considered in this study for all the essential terminology are presented in Supplementary Table 1.

## **3. Stepwise framework for quantification of primary forestry residues**

*Table 1* highlighted that efforts have already been undertaken to develop methodologies to spatially estimate the PFRs. The approach used here builds upon the existing efforts, and in particular, upon the landmark BEE handbook technique presented in Vis and Van den Berg [31], also used as an underlying framework for many of the studies carried out post-2010 (Table 1).

However, unlike [31], an in-depth focus on the specific PFR stream and high spatial resolution is made, data uncertainty and its propagation throughout the calculation process are incorporated, and the use of the methodology is exemplified via a national case study. This translates into a 4-step methodology, here referred to as the CamBEE method for spatial quantification of PFRs (Figure 2).

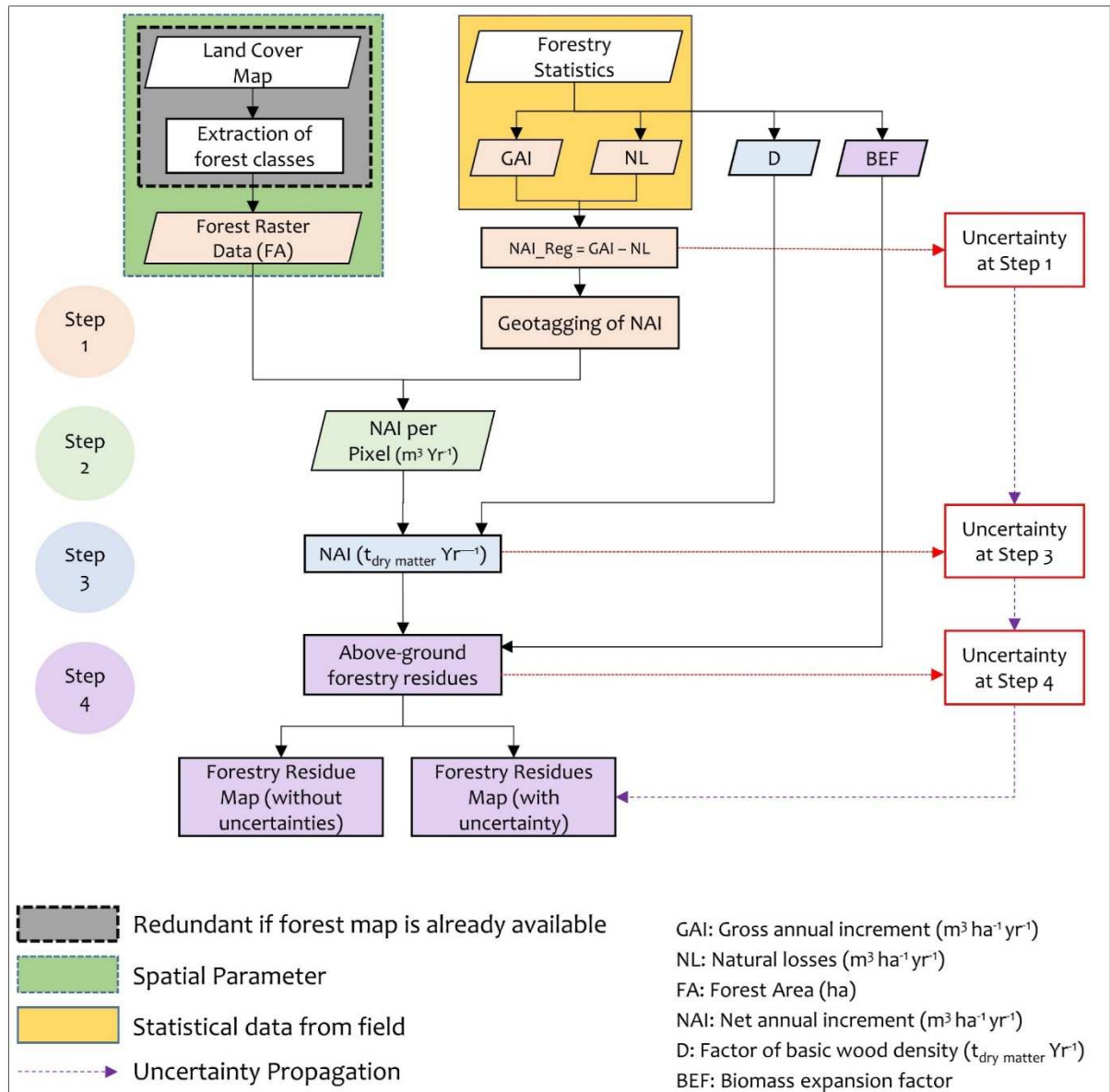


Figure 2: Generic CamBEE stepwise framework for estimating the primary forestry residues with uncertainty quantification

#### Step 1: Spatially-explicit increment statistics

The first step in the spatial quantification of PFRs involves the spatial estimation of the NAI, which is one of the key input parameters. The NAI provides an indication of the average biomass growth and productivity in a forest. NAI is mathematically defined as the average merchantable annual volume gained over the given reference period, also referred to as Gross Annual Increment (GAI), minus the natural losses (NL) on all trees (see definitions of Supplementary Table 1), as shown in Eq. (1):

$$NAI_{reg} = GAI_{reg} - NL_{reg} \quad \text{Eq. (1)}$$

Where:  $NAI_{reg}$  is the annual merchantable stemwood increase per region based on inventory statistics ( $\text{m}^3 \text{ha}^{-1} \text{year}^{-1}$ ),  $GAI_{reg}$  is the regional gross annual increment ( $\text{m}^3 \text{ha}^{-1} \text{year}^{-1}$ ), and  $NL_{reg}$  is the average natural losses ( $\text{m}^3 \text{ha}^{-1} \text{year}^{-1}$ ) per region, based on inventory statistics. It should be noted that in an endeavor of harmonization, these notations are kept exactly as they appear in the BEE method [31]. The term region is here understood as the area for which the GAI and NL data are available.



The values of  $GAI_{reg}$  and  $NL_{reg}$  can be retrieved from forestry statistical data, e.g., from NFIs, which are now compulsory in the EU [34]. Furthermore, all ‘Annex 1’ countries of the Kyoto Protocol [35] (36 in total) are mandated, since 2000, to publish their national greenhouse gas emission inventory report online [36] (so-called NIR reports), from which  $GAI_{reg}$  and  $NL_{reg}$  can also be retrieved (at best) or else extrapolated. Alternatively, in regions where this data is not available, the value of  $NAI_{reg}$  can be estimated from Net Primary Productivity (NPP) maps derived from satellite observations [31,37].

#### Step 2: Fusion of regional NAIs and forest map

In the second step (Figure 2), the  $NAI_{reg}$  values are assigned to the actual forestland. This is accomplished by fusing a forest map raster of the area under assessment with the average stemwood NAI per region ( $NAI_{reg}$ ) obtained at step 1, in order to get the average stemwood NAI per pixel. The calculation is made as per Eq. (2);

$$SW\_NAI = FA \times NAI_{reg} \quad \text{Eq. (2)}$$

Here,  $SW\_NAI$  is the raster of average stemwood NAI per pixel ( $m^3 \text{ year}^{-1}$ ), and  $FA$  is a raster of forest area (ha), obtained from forest maps. The forest map of the area under assessment can be obtained from land-cover data, NFIs, or earth observation data. The forest map provides an understanding of how many hectares of land is under forest with their exact location. Vis and Van den Berg [31] recommend using the forest data with the best possible spatial resolution to get the highest accuracy. Apart from NFIs, this data can be derived from other data platforms such as Global Land Survey (GLS) [38], Climate Change Initiative (CCI) Land Cover V2 [39], GlobeLand30 [40], CORINE Land Cover (CLC) [41], etc., unless finer regional data can be obtained.

Furthermore, for the GIS operation in step 2, the input data ( $FA$  and  $NAI_{reg}$ ) should be of the same data type (either shapefile or raster). In cases where one data is different, then data should be converted to the same format. In addition, care should be taken to harmonize the output cell size (pixel size) for both input parameters.

#### Step 3: Conversion from volume to mass

In the third step, the increment information obtained from step 2 is converted to tonnes dry matter (megagrams dry matter:  $Mg_{dry \text{ matter}}$ ), by multiplying the increment volume and the factor for basic wood density as per Eq. (3);

$$SW\_NAI\_t = SW\_NAI \times D \quad \text{Eq. (3)}$$

Here,  $SW\_NAI\_t$  is the raster of the average stemwood net annual increment ( $Mg_{dry \text{ matter}} \text{ year}^{-1}$ ), and  $D$  is the wood density ( $Mg_{dry \text{ matter}} \text{ m}^{-3}$ ). It should be noted that the value of  $D$  is unique for every species. The IPCC Good Practice Guidance handbook [42], provides the values for basic wood density for particular species of different forest types (Boreal, Temperate, Tropical) and specifies the sources of this data. These values are usually an average of different observations for a particular specie, usually withdrawn from a handbook or, in some cases, derived from regression equations such as the one in Reyes et al. [43]. When forest maps do not include details about the particular tree species, the BEE method suggests applying average wood density factors at the regional level.

#### Step 4: Aboveground biomass

Usually, forest inventories do not measure crown biomass (leaves, twigs, needles, branches), but rather the diameter (at breast height) and height of trees, which is then translated into “stemwood”, i.e., the round wood that results from harvesting. As a result, the aboveground biomass produced above X-meter of height (in the form of leaves, twigs, needles, branches) is seldom measured but estimated. This implies that the contribution of these aboveground residues is not registered in the increment raster layer defined in Eq. (3). In inventories, the biomass from leaves/needles, twigs, and branches is typically estimated from the NAI with Biomass Expansion Factors (BEF). BEF expands the dry-weight of the growing stock or net annual increment to include the non-merchantable components of the tree, stand, or forest [44]. Usually, the BEF is considered as constant or species/area-specific values, but in reality, they are variables [45].

Subsequently, in the final step for estimation of PFRs, the raster of biomass increment in foliage and branches is created by fusing the stemwood increment raster ( $SW\_NAI\_t$ ) with related BEF for aboveground biomass as per Eq. (4). In Eq. (4), the stemwood increment is subtracted from its product with BEF to produce a raster layer that only includes the information on aboveground forestry residues.

$$AGFR\_AAI\_t = (SW\_NAI\_t \times BEF\_Above) - SW\_NAI\_t \quad \text{Eq. (4)}$$

Here,  $AGFR\_AAI\_t$  is the raster of average annual increment in biomass from aboveground forestry residues ( $\text{Mg}_{\text{dry matter}} \text{y}^{-1}$ ), and  $BEF\_Above$  is the average biomass expansion factor for conversion of annual net increment to aboveground tree biomass increment. Here, the notation  $BEF\_Above$  is simply used in conformity with the notation used in the BEE technique by Vis and Van den Berg [31]. According to Schoene et al. [46], BEF, as withdrawn from the IPCC 2006 guideline (Specifically, Table 3A.1.10), is used for estimating the whole tree aboveground biomass only. The values for BEF represent averages for average annual increment or age and is provided as a constant parameter with ranges. The young forest with low growing stock is represented in the upper limit of the range, and the lower limit of the range approximates the mature forest with high growing stock.

### 3.1 Uncertainty assessment and propagation:

Usually, environmental data for large geographical scales are assessed by sample-based techniques, as the accounting of each tree population is not economical or technically feasible. Statistically, in a sample-based survey, a subset of samples from the population is used to estimate the population parameters based on probability theory. These estimated parameters may differ from the true values as they might be affected by errors such as; sampling errors, assessment errors, including classification and measurement errors, prediction errors induced by models, and non-statistical errors [47]. Such errors are common to all assessments and monitoring programs, and these errors have been examined exhaustively in different studies [48–51]. Statistically, measurement errors can be categorized into two groups: systematic errors and random errors. The systematic error that is also referred to as bias is represented as a fixed value for the discrepancy with the true value and is directly related to the accuracy of an estimate. Theoretically, a systematic error can be eliminated from the result by using an appropriate correction factor [52]. However, in sample-based surveys, the presence of bias, which is the lack of accuracy, is often unknown, and using a correction factor may introduce an additional uncertainty associated with that corresponding correction factor. Random error, on the other hand, indicates that the error changes over the period of measurement, or may be transferred from one set of measurements to the other. The range of these changes is a measure of the uncertainty created by these errors. In this study, the focus was on estimating the uncertainties only associated with the random errors of measurement.

From Figure 2, it can be observed that the final output is determined by establishing three functional relationships, where the output of the preceding step is the input for the successive step. When parameters are derived through a series of functional relationships, the uncertainties in the inputs of these functions will propagate through the calculation, in the form of random errors [53]. These uncertainties were accounted for based on state-of-the-art uncertainty propagation techniques, as comprehensively detailed in the work by Farrance and Frenkel [54], and the standard guide to expression of uncertainty in measurement [53].

The first step in the uncertainty assessment deals with the propagation of uncertainty in the calculation of  $NAI\_reg$  through Eq. (1). As the input variables ( $GAI\_reg$  and  $NL\_reg$ ) are uncorrelated, the standard uncertainty for the function in Eq. (1) should be evaluated in the following step, using Eq. (5), since Eq. (1) can be represented by a generic function  $y = x_1 - x_2$ , where  $x_1$  and  $x_2$  are uncorrelated. For such function, as per the Guide to Uncertainty and Measurement (GUM) [53], the uncertainty can be expressed as:

$$u^2(y) = u^2(x_1) + u^2(x_2) \quad \text{Eq. (5)}$$

Here,  $u^2(y)$  is the squared standard uncertainty (numerically and mathematically equal to variance) in  $y$ , and  $u^2(x_n)$  is the standard uncertainty squared for a given  $x$  variable. The variable  $x_1$  here corresponds to the  $GAI\_reg$  values, and the variable  $x_2$  corresponds to the  $NL\_reg$  values. For cases where the standard deviation of  $NAI$  is

provided, uncertainty propagation using Eq. (5) would be redundant, and the uncertainty assessment should then start from the next step.

The uncertainty from Eq. (5) is then propagated to the calculation of average stemwood  $SW\_NAI\_t$  in  $Mg_{dry\ matter}\ year^{-1}$  through the functional Eq. (3). To account for the uncertainty in the functional Eq. (3), the expression giving the standard uncertainty in Eq. (6) was used, since Eq. 3 is a function that can be expressed as  $y = Ax_1$ , where 'A' is a constant, and  $x_1$  is a measured variable. Accordingly, the uncertainty can be expressed as:

$$u^2(y) = A^2u^2(x_1) \quad Eq. (6)$$

In this equation,  $u^2(y)$  is the squared standard uncertainty in the measurand  $y$  (*here*  $SW\_NAI\_t$ ), and  $u^2(x_1)$  is the standard uncertainty squared for the variable  $x_1$ , *here*  $SW\_NAI$  that is propagated through Eq. (5). The constant  $A$  corresponds to the factor of basic wood density ( $D$ ). The value of  $D$  is considered as a constant and represents the mean density for different tree species of a particular forest class. To evaluate the uncertainty coming from the range of  $D$ , Eq. (6) is here calculated with the maximum and  $D$  values.

Finally, the uncertainty from Eq. (6) is propagated in the calculation of aboveground forestry residues. Eq. (4) has two arithmetic operations, and its generic structure is  $y = Ax_1 - x_1$ . Therefore, the uncertainty for this step is evaluated in two stages. The first stage follows the uncertainty expression in Eq. (6), and the second stage follows the uncertainty expression in Eq. (5). To begin with, the first stage relates to the  $SW\_NAI\_t$  parameter and to the BEF constant. As for the density, the calculation is conducted by incorporating the maximum and minimum values of BEF, in order to encompass the entire range of the BEF in the uncertainty. In the second stage, the data incorporating the uncertainties from the total annual aboveground biomass ( $BEF \times SW\_NAI\_t$ ) is merged with the uncertainty of the merchantable aboveground biomass ( $SW\_NAI\_t$ ; in  $Mg_{dry\ matter}\ year^{-1}$ ). This ultimately provides the uncertainty that gets propagated in the spatial quantification of aboveground forestry residues.

Here, there are two non-constant statistical input variables of forestry from which uncertainty propagates, viz.,  $GAI\_reg$  and  $NL\_reg$  (or  $NAI\_reg$  if NAI is directly available). Ideally, the standard deviation associated with these values will be provided (or the raw measurement datasets to derive it), and this can be used as the value of "u" in Eqs. 5-6. In cases where no indications of the standard deviation are provided, techniques are available to derive an uncertainty. Notably, the pedigree matrix technique [55] was developed in the field of life cycle assessment, where such a situation is common.

#### 4. Exemplification of the use of the CamBEE method

##### 4.1 Study Area

To exemplify the proposed technique, a case of Metropolitan France was presented (Mainland European France, including Corsica), herein referred to as France. France is administratively divided in the following hierarchy: Regions (13) > Departments (96) > Communes (36569), though other administrative or political areal units also exist. In terms of the latest European Nomenclature of Territorial Units (NUTS), Regions correspond to the NUTS level 1 level while Departments correspond to NUTS level 3 [56].

France is a key country for the European bioeconomy [57] and accounts for almost 10% of the European forest cover and has the fourth largest forest area in the EU behind Sweden, Finland, and Spain [58]. In France, forests cover approximately 168000  $km^2$  or about 30.8% of the total French territory and are dominated by Temperate and Mediterranean type forests [59]. About 76% of the total forest in France is privately owned (**ca.** 64% by individuals and families and 12% by private industries) [60]. The remaining 24% of the forests are owned by the French government, out of which about 14% is communal (belonging to the municipal or other local authorities), and 10% is provincial (belonging to the state) [59,60]. The public forests nevertheless account for 40% of the timber harvest [61]. In the present exemplification, the annual availability of PFRs for both privately owned and public forests were determined. The vision is that this may serve as a piece of key information to facilitate eventual decisions related to the mobilization of PFRs from the perspective of national bioeconomy strategies. Additional details on French forestry are available in the supplementary materials.

To estimate aboveground PFRs, the CamBEE method requires five main input data, viz., the forest cover raster; forest statistics on gross annual increment (GAI) and natural losses (NL) if net annual increment (NAI) is not available per region; factor of basic wood density (D), and biomass expansion factor (BEF). Other ancillary data required for mapping are the administrative shapefile (e.g., country or regional boundary). The source of data used in the present study is provided in *Table 2*.

*Table 2: Source of data used in the present study*

Data Type	Used for	Source	Time scope
Forest Cover	Used in Step 2 of the CamBEE process	[62]	2007 - 2018
Forest Inventory Statistics	Used in Step 1 of the CamBEE process	[63]	2011 - 2015
Biomass Expansion Factors (BEF)	Used in Step 4 of the CamBEE process	Table 3A.1.10; [42]	<2003 <sup>+</sup>
Factor of basic wood density (D)	Used in Step 3 of the CamBEE process	Table 3A.1.9-1; [42]	<2003 <sup>+</sup>
Administrative shapefile	Used in the exemplification section	[64]	-
EPCI <sup>1</sup> Shapefile	Used for extracting the inventory statistics data in the exemplification	[65]	-
Public / Private forest shapefile	Used for identifying the publicly owned and the privately owned forests of France in the exemplification section	[66]	-

<sup>1</sup> A French administrative regional unit that groups several communes based on some of their common competences. There are 1258 EPCI in France (as of 1<sup>st</sup> January 2019). This was needed since the data supplied for NI\_reg and GAI\_reg were supplied at the EPCI level only.

<sup>+</sup> The values of BEF for different forest types were obtained from the IPCC good practice Guidance report [42], which remained unchanged in the recent 2019 IPCC refinement of the 2006 guidelines for national greenhouse gas inventory [67]. The report takes these values from several references that are from the 1990s. For D, as these values are specie-specific, their values in the IPCC report was also taken from several references, some of which were from 1968.

For the present study, the BD Forest® V2 data [62] was used for FA. The BD Forest® V2 data is the most comprehensive forest data in France, which can be downloaded in vector (GIS) format and contains 32 forest classes based on a hierarchical structure. These were aggregated to three forest classes (Conifers, Broadleaf, and Mixed), as illustrated in Figure 3. An example of aggregation for the Occitanie region of France is shown in Supplementary Figure 1.

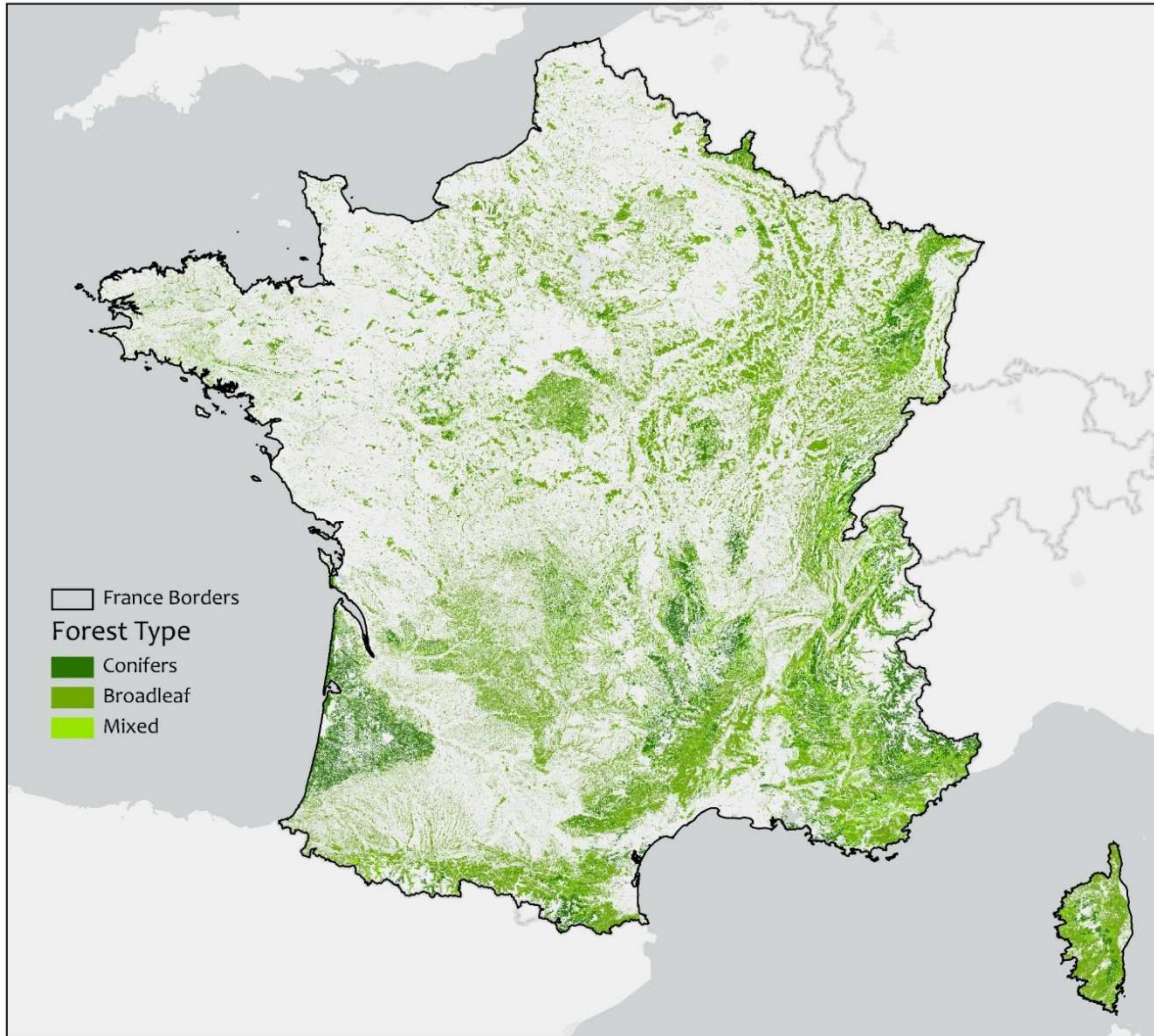


Figure 3: Aggregated forest map of Metropolitan France to 3 forest types

The statistical data on GAI\_reg and NL\_reg (step 1) was retrieved from [63,68], a dataset built for a national tool called ALDO, which provides an estimate of carbon sequestration in soils and biomass. The ALDO tool contains data on production and mortality among others for conifers, broadleaf and mixed forest types at the French EPCI administrative level. The statistical data from the ALDO tool for every EPCI were added to the administrative EPCI shapefile and converted to the raster format for further processing (step 2). This step was facilitated with the polygon to raster tool in ArcGIS Pro. In this step, the cell (or pixel) size of the forest raster is determined.

Although the ALDO dataset provided the required GAI\_reg and NL\_reg data, it did not provide the uncertainty ranges or the standard deviation of these variables. The standard deviation for the calculated NAI was estimated using the standard deviation classification method in ArcGIS Pro [69]. The standard deviation classification method estimates how much the value of the NAI of a given area (here EPCI) varies from the mean of all areas considered. The calculated standard deviation value was thus used as a proxy for the standard uncertainty value of NAI\_reg instead of using Eq.5. Of course, the standard deviation classification method of ArcGIS Pro could have been used to derive a proxy standard deviation for both GAI\_reg and NL\_reg, and these uncertainties could have been propagated as in Eq.5. Yet, this was seen to induce artificial uncertainty, therefore, the proxy standard uncertainty obtained on NAI\_reg was directly considered, and used for the next steps. For D and BEF, the uncertainty ranges provided in the IPCC [42] were used. From this, a low and high spatial estimate of PFRs was calculated using Eq. 5-6, as described in section 3.1.

## 4.2 Deciding the spatial resolution

The main objective of this study was to develop an easily replicable method for high-resolution spatial quantification of aboveground PFRs at the pixel level. Here, high-resolution corresponds to high spatial resolution, the definition of which is provided in Supplementary Table 1. Over the years, due to the improvements in satellite products and processing techniques, this definition has kept on evolving. For example, what was considered as high-resolution in the 1980s (LANDSAT 60-meter / pixel), has become low in today's standards. Typically, the resolution of any spatial study is based on the type of data available and the study purpose. For example, in the study by Hansen et al. [70], high-resolution global maps were produced using Landsat data at a 30-meter spatial resolution to characterize the forest extent, loss and gain from 2000 to 2012. Further research by Inglada et al. [71] reported using Landsat 8 data (30-meter / pixel) for producing high-resolution land cover maps at the country scale (France). It may be argued that as per current standards, a resolution of 30-meter corresponds to a medium resolution, while high spatial resolution would range anywhere from 10-meter to the minimum extent possible [72]. On the other hand, the scale or geographic extent of the study is a key determining factor in defining what can be considered as a high-resolution or not. Furthermore, creating land cover maps using high-resolution satellite imagery (< 10-meter) has multiple cons. These include high costs, as commercial satellites carrying the most advanced sensors are expensive; Small coverage area or swath, as the higher the resolution, the less total ground area can be covered in a scene. Contrarily, low spatial resolution data contain lower level of details which might not be suitable for supporting local bioeconomy decisions.

As there are no standard procedures to decide what spatial resolution would be ideal for spatial quantification of PFRs at the country scale, a metric based on computational complexity is here proposed (in terms of size of data and processing time). To test the deviation of estimated results at different spatial resolutions, the theoretical potential of aboveground PFRs of conifer forests in the Occitanie region was evaluated. The conifer forest of the Occitanie region was sampled at the spatial resolution of 100-meter, 30-meter, 20-meter, 10-meter, 5-meter, and 1-meter (step 2).

Figure 4 shows the generated forest raster at different spatial resolutions overlaid on a base map. Figure 4 highlights that the coarser-resolution data, especially the 100-meter one, may mask other land cover types. At the same time, resolutions of 20-meter and below are less likely to mask other land cover types. On the other hand, the sampling of large vector datasets to smaller cell sizes may excessively enhance the computational budget in terms of processing time and storage [73]. This can be witnessed in Figure 5, where the processing time and the space requirement increases at a logarithmic scale, especially for the data being processed at less than 10-meters. The conversion of complex forest shapefile (Vector) to raster at 1-meter resolution took 20475 seconds, compared to 34 seconds for the same data at 10-meter resolution, which is nearly 600 times more. Similarly, the size of the processed raster image was nearly 80 times more for the 1-meter sampled data (0.96 gigabytes) compared to the 10-meter one (0.012 gigabytes). The final uncompressed size of the processed raster containing information on the location and quantity of PFRs for the conifer forest of the Occitanie region was 490 gigabytes for the 1-meter resolution data (Supplementary Table 2). The values highlighted in bold in Figure 5 show the increase in the complexity in terms of time per pixel area and file size per pixel area. There is a substantial increase from 10-meter spatial resolution data to 5-meter data for both processing time and file size. This test was performed only for one forest type of one region of France; thus, the estimation of PFRs for the entire country at a very high spatial resolution would be rather tedious.

Supplementary Table 3 shows the results of the theoretical potential of aboveground PFRs (Conifers) for different departments of the Occitanie region in  $\text{Mg}_{\text{dry matter}} \text{ year}^{-1}$  at different spatial resolutions. A pairwise comparison was then made to establish the percentage difference in the results of spatial quantification at different resolutions. This illustrates that for most of the cases, the percentage difference in estimation was marginal (> 0.2%). In view of these results, it was decided to select 10-meter as the most optimal resolution based on the computational budget and comparison with other resolutions.

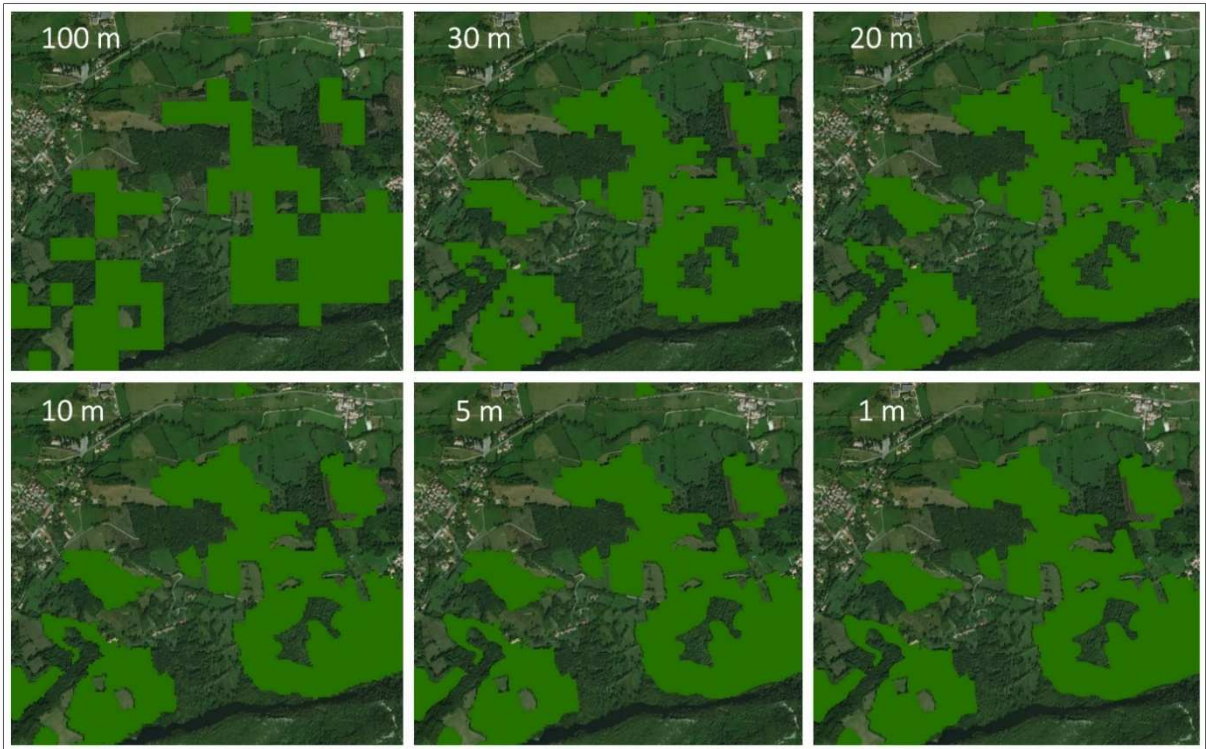


Figure 4: Visual representation of different spatial resolutions for conifers in a given area of the French Occitanie Region. The areas in light green are the areas considered to be conifer forest, for the selected resolution.

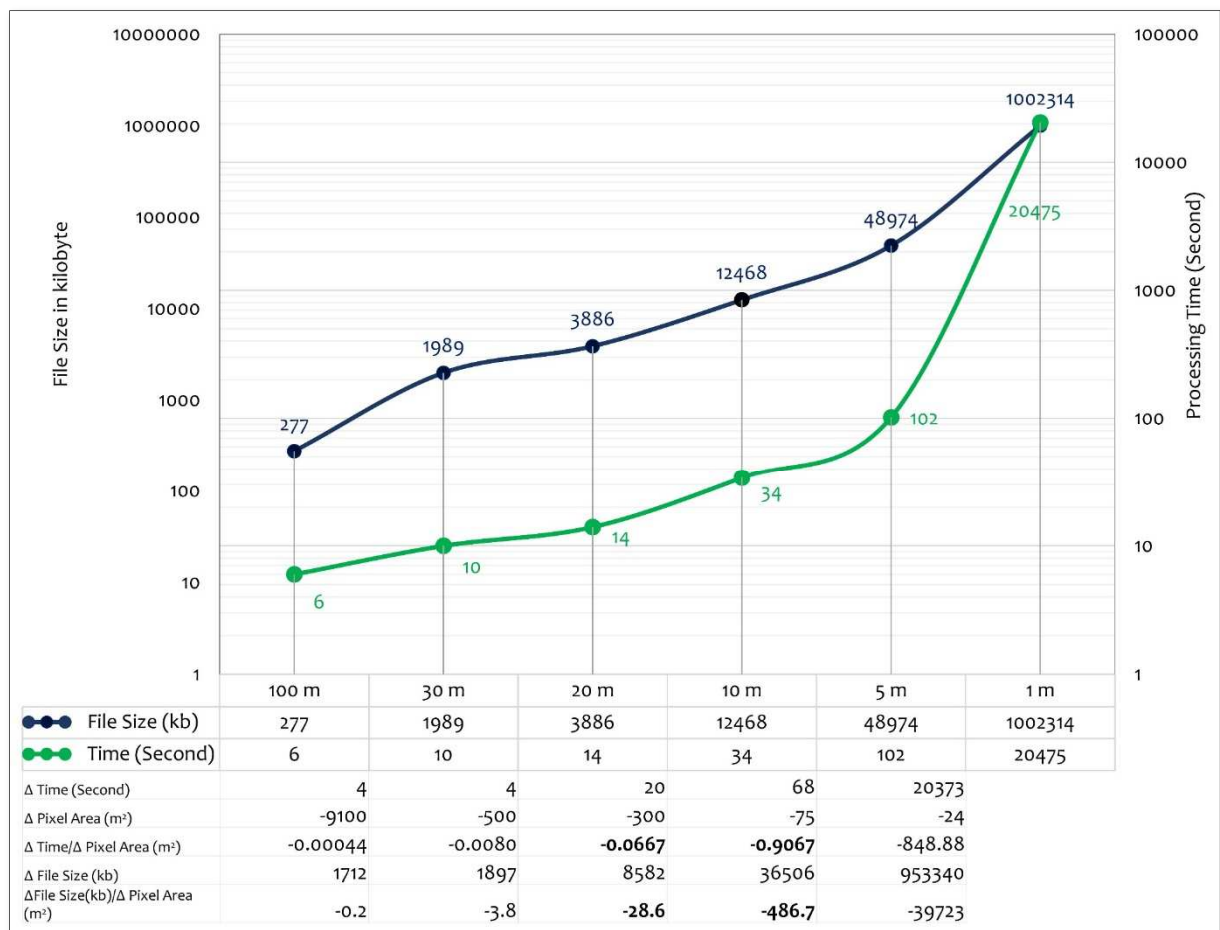


Figure 5: File size and processing time at different spatial resolutions. The labels on the x-axis are qualitative and represent the size of a pixel (e.g., 100 m corresponds to an area of 100<sup>2</sup> m<sup>2</sup>)

#### 4.3 Exemplification results

Figure 6 shows the theoretical potential of PFRs for France in terms of Mg<sub>dry matter</sub> year<sup>-1</sup>. The spatial quantification result is illustrated in the form of 10-meter x 10-meter pixels (100 m<sup>2</sup>), which is, to the author's knowledge, the first-ever high-resolution map of available potential of PFRs at a country scale. The advantage of using discrete high-resolution pixels is that it allows for aggregation of these pixels at different administrative levels, such as regions or departments. The theoretical potential for PFRs in France, when observed at the pixel level (here 100 m<sup>2</sup> per pixel), varies from ≤ 0.15 Mg<sub>dry matter</sub> year<sup>-1</sup> per pixel to a maximum of 0.91 Mg<sub>dry matter</sub> year<sup>-1</sup> per pixel. From Figure 6 it can be observed that the residues are mainly concentrated in the Mediterranean basin in the regions of Occitanie and Provence-Alpes- Côte d'Azur, the Landes forest in the south-western part of the country in the Nouvelle-Aquitaine region, the east of the country in the Grand-Est and Bourgogne-Franche-Comté regions and in the mountainous region of Auvergne-Rhône-Alpes. The regions in the north and north-west of France have scattered PFRs, reflecting the forest structure in these regions. The island region of Corse, despite having the highest concentration of forests in terms of total percent cover of land area (Supplementary Table 4), produces a rather low quantity of residues per pixel (0.15 – 0.45 Mg<sub>dry matter</sub> year<sup>-1</sup> per pixel) in comparison to other French Regions. From a mechanistic viewpoint, the only variable that contributes to the quantity of residues being lower in this region is the annual increment. Similarly, the south-eastern and southern parts of France, especially in the Mediterranean basin, have a lower quantity of PFRs, ranging from ≤ 0.15 Mg<sub>dry matter</sub> year<sup>-1</sup> to 0.30 Mg<sub>dry matter</sub> year<sup>-1</sup> per pixel.



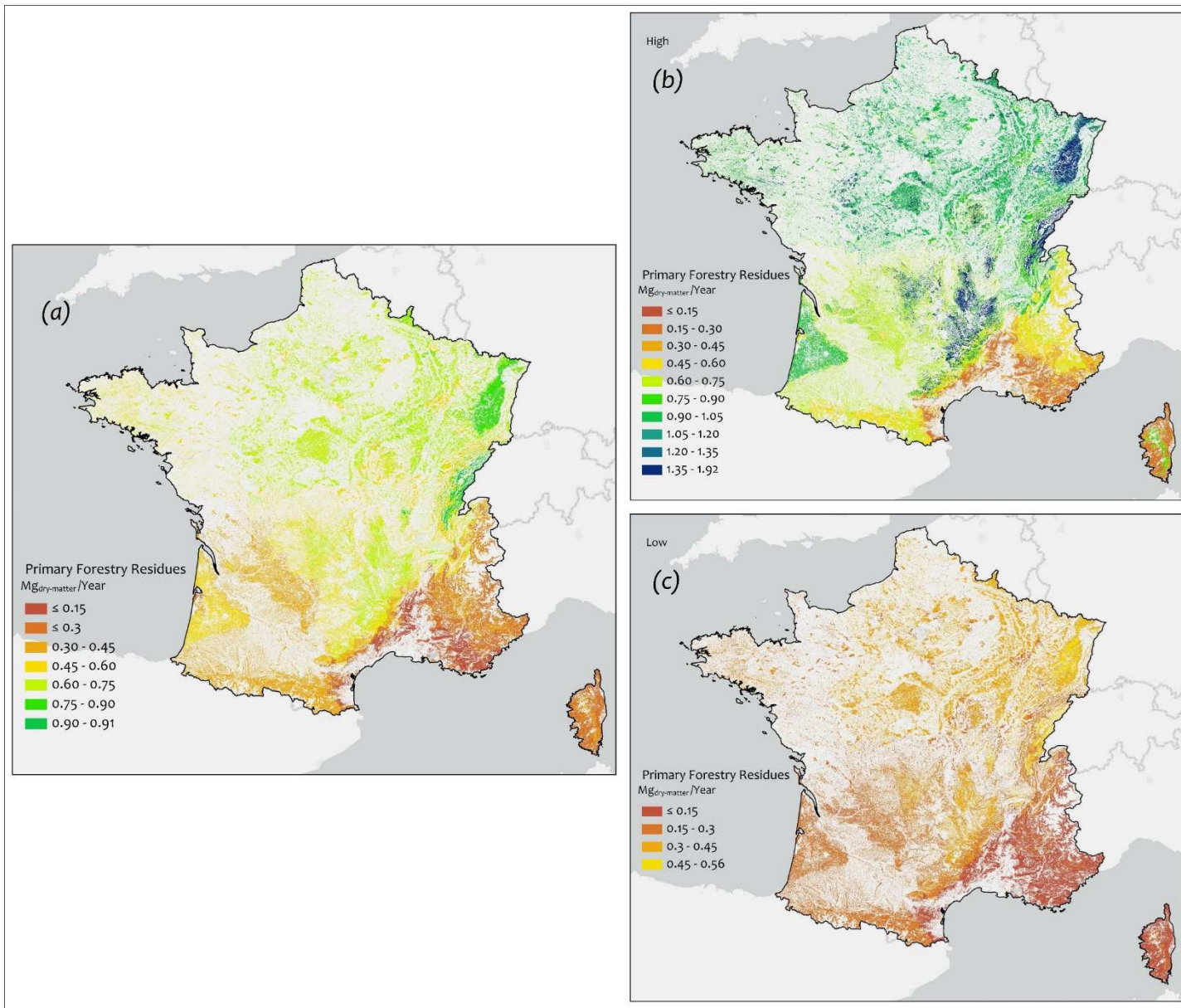


Figure 6: Theoretical annual potential of (a) average primary forestry residues (b) with maximum ranges (c) and minimum ranges at a harmonized scale

Supplementary Figure 2 shows the aggregated distribution of PFRs in terms of Million  $\text{Mg}_{\text{dry matter}} \text{ year}^{-1}$  to the departmental and the regional administrative levels, while Table 3 shows the overall theoretical potentials per region. The total theoretically available potential of PFRs in France is about 8.4 Million  $\text{Mg}_{\text{dry matter}} \text{ year}^{-1}$ , ranging between 4.4 Million  $\text{Mg}_{\text{dry matter}} \text{ year}^{-1}$  with the lower values of the uncertainty range and about 13.9 Million  $\text{Mg}_{\text{dry matter}} \text{ year}^{-1}$  with the higher values of the uncertainty range. The departmental distribution of PFRs is presented in Supplementary Table 5. The Vosges department in the region of Grand-Est has the greatest availability of PFRs at about 0.235 Million  $\text{Mg}_{\text{dry matter}} \text{ year}^{-1}$ . All of the regions showed an important fluctuation of estimated PFRs between the lower range and higher range values, and nearly all of the higher values were approximately three times more than the lower values for all regions (Table 3).

Supplementary Figure 3 illustrates the distribution of PFRs for private and public forests in France. A clear distinction can be made in the spatial distribution of these resources, as private forests are evenly spread across France compared to the public forests which are concentrated in the region of Grand-Est and other mountainous regions covering the French Alps and the Pyrenees. Private forests have a larger share of forestland, which naturally produce more forestry residues compared to the public forests. The ratio of produced PFRs for private and public forests is almost 3:1. The cumulative amount of PFRs available from private forests in a year is almost 6.2 Million  $\text{Mg}_{\text{dry matter}}$ , compared to approximately 2.1 Million  $\text{Mg}_{\text{dry matter}}$  for public forests (Table 3).

Table 3: Overall PFRs produced per region, in Million  $\text{Mg}_{\text{dry matter}} \text{ year}^{-1}$

Region Name	Million $\text{Mg}_{\text{dry matter}} \text{ year}^{-1}$				
	Available Potential	Lower Range	Higher Range	Private Forests	Public Forest
Auvergne-Rhône-Alpes	1.316	0.708	2.292	1.067	0.249
Bourgogne-Franche-Comté	1.160	0.603	1.894	0.710	0.450
Bretagne	0.267	0.138	0.437	0.248	0.019
Centre-Val de Loire	0.601	0.307	0.947	0.531	0.070
Corse	0.132	0.069	0.219	0.100	0.032
Grand Est	1.335	0.696	2.194	0.587	0.748
Hauts-de-France	0.287	0.146	0.442	0.216	0.071
Île-de-France	0.177	0.090	0.273	0.124	0.053
Normandie	0.263	0.135	0.415	0.207	0.056
Nouvelle-Aquitaine	1.209	0.647	2.068	1.113	0.096
Occitanie	1.113	0.583	1.837	0.900	0.213
Pays de la Loire	0.206	0.109	0.341	0.187	0.019
Provence-Alpes-Côte d'Azur	0.343	0.185	0.608	0.227	0.116
<b>Total</b>	<b>8.409</b>	<b>4.416</b>	<b>13.966</b>	<b>6.217</b>	<b>2.191</b>

A standard uncertainty map (Figure 7) was also synthesized after estimating the higher and lower values of PFRs. The pixels in the standard uncertainty map of PFRs represent the uncertainty in terms of  $\text{Mg}_{\text{dry matter}} \text{ year}^{-1}$  per pixel. The standard uncertainty of availability of PFRs in France,  $u(AGFR\_AAL\_t)$ , ranged from a minimum of 0  $\text{Mg}_{\text{dry matter}} \text{ year}^{-1}$  to a maximum of 0.68  $\text{Mg}_{\text{dry matter}} \text{ year}^{-1}$ . From Figures 6 and 7, it can be observed that the uncertainty is observed to be higher in areas where the available potential for PFRs is also high and lower in areas where the available potential for PFRs is smaller.

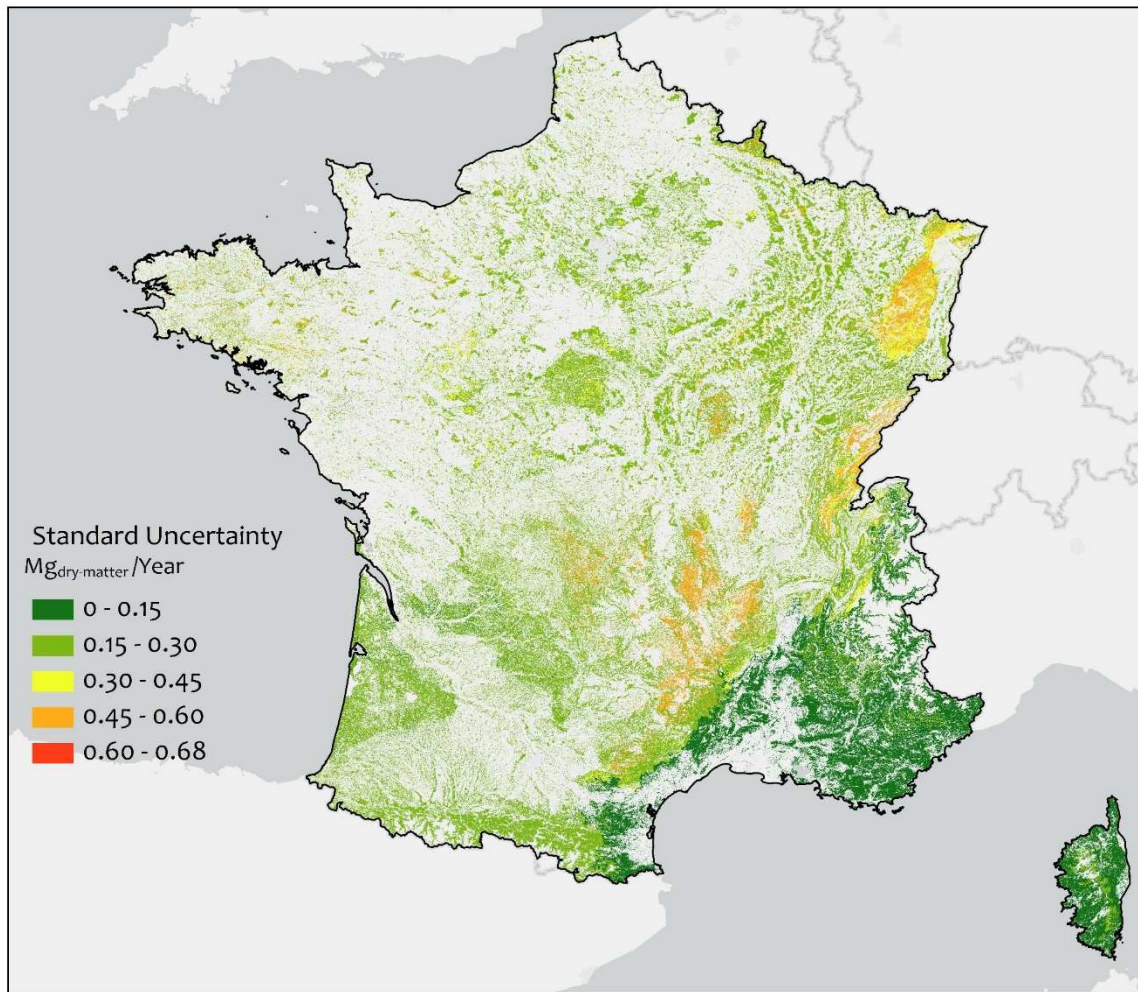


Figure7: Standard uncertainty in the estimation of Primary Forestry Residues at the pixel level

## 5. Discussion

The work presented in this study bridges the gap between spatial sciences, forestry, and bioeconomy by providing an easily replicable spatially-explicit framework “CamBEE” for estimating PFRs at high-resolution. By being at the intersection of geographical and “bioeconomic” science, it is also the first attempt to discuss questions such as the appropriate resolution for these types of assessments. The CamBEE framework can work across wide ranges of geographical scales and spatial resolution with open-source data. The study also provides a detailed illustration of the proposed framework and exemplifies its use as a case study for France. What makes the CamBEE framework unique is the explicit incorporation of uncertainties to derive the final PFR estimates. The other existing methods (Table 1) do not account for the uncertainty that may be incorporated through the input data or that are propagated through the calculation steps. The exemplification case for France highlighted that the variability of estimates can reach a relatively high degree; a theoretical PFRs potential ranging from about 4.4 Million  $\text{Mg}_{\text{dry matter}} \text{ year}^{-1}$  to about 13.9 Million  $\text{Mg}_{\text{dry matter}} \text{ year}^{-1}$  was obtained (i.e., ca. doubling or halving the potential estimated without uncertainties). The difference between the lower and the higher ranges of the estimate ( $9.5 \text{ Mg}_{\text{dry matter}} \text{ year}^{-1}$  or  $182.3 \text{ PJ year}^{-1}$  based on a lower heating value (LHV) of  $19.19 \text{ GJ Mg}^{-1} \text{ DM}$ ) alone is almost equivalent to about 2.8% of the total energy consumption of France in 2017 [74]. Therefore, the uncertainty must be accounted for when making strategic investment decisions concerning future bioeconomy technologies.

The framework presented and illustrated in this paper can be used to derive the theoretical potential of PFRs. However, as the framework is explicitly described, different restriction conditions can easily be applied within the Geographic Information System (GIS) environment that can be used to yield other potentials. These would then be considered as a step 5 of the CamBEE framework. In fact, some studies express concerns with the maintenance of soil organic carbon as an important ecological service provided by PFR residues [7]. Though essential for bioeconomy strategies [6,75], quantifying the difference of environmental impacts between the

current and potential use of PFR is obviously beyond the scope of the present study, but such assessment can henceforth be made at a spatially-explicit scale using the CamBEE framework.

Moreover, because it is transparent and builds upon open-source data, the CamBEE framework can easily be used by any authorities, planners, or stakeholders worldwide for the area level they are interested in. This, of course, requires basic GIS skills, which are typically accessible in planning entities. As such, the major implication of this study is that there is now a tool available for bioeconomy planners for quickly quantifying at a high-resolution level the availability of PFR, along with the uncertainty of this estimate.

The exemplification results of the case study can be validated, at least partially, using the statistical data published by Colin and Thivolle-Cazat [76]. In their study, the authors report what they refer to as “gross availability” (similar to theoretical potential) for branches and twigs <7 cm, which roughly translates to PFRs (excluding the foliage) around 6.08 Million  $\text{Mg}_{\text{dry matter}} \text{year}^{-1}$  for the years 2016-2020. This data is not directly available in [76] as the values for gross availability are provided in  $\text{m}^3 \text{year}^{-1}$ , but these can be converted to mass using the IPCC factors of basic wood density [42]. The final estimated figure for France thus deviates by ca. 38% from the national statistical data; here it is not claimed as a proof of validation, but it builds confidence around the range found with CamBEE.

In contrast, the spatially-explicit study of Hamelin et al. [4], where estimates are reported at the European NUTS level 3, reveal a theoretical potential of 455  $\text{PJ year}^{-1}$  for PFR in France (results extrapolated from the raw dataset of the authors). This represents ca. 24 Million  $\text{Mg DM year}^{-1}$ , based on a lower heating value (LHV) of 19.19  $\text{GJ Mg}^{-1} \text{DM}$  [8], which is nearly 3-fold the potential found in the present study. The higher value reported in [4] is explained by (i) the inclusion of stumps as a residual component of the stream, and (ii) the methodological framework itself, where country-level data on forest statistics were simply (and coarsely) scaled down to different administrative regions. Conversely, the present framework aggregates pixel-level data to different administrative regions following a bottom-up approach, thus avoiding inconsistencies in the resolution of the dataset used, and providing more reliable estimates. This indicates that the results of [4] may be overestimated, and accordingly that the residual biomass potential generated in Europe might be lower than previously anticipated.

The results obtained from the CamBEE framework are only as good as the input data supplied. Although the uncertainty assessment tries to capture the deviation as ranges, uncertain data will make this range large. In the exemplification section, the forest increment statistics that are derived from [63] uses the statistical data of the French intercommunal plans for energy and climate (PCAET; [68]), which in turn cross-reference the NFI survey data with the 11 French Biome Regions (GRECO; [77]) and the French Forestry Regions (SER; [77]) data. The GRECO and SER data describe the climate, geology and geomorphology, hydrography, soils, vegetation, land-use, and forest landscape. The common spatial pattern irrespective of the numerical ranges in the derived maps of France follows the same spatial pattern of the GRECO and SER. The question of how this imposed spatial pattern affects the actual availability of PFRs on the field remains unanswered and can only be verified by extensive field sampling.

Furthermore, it should be highlighted that the results obtained from the CamBEE framework are a representation of the past. In the case study, data from different periods have been used, e.g., the forest map is developed by combining field data from multiple observations at different places with remote sensing data on forest structure (Table 2). The statistical data on the factor of basic wood density and biomass expansion also stem from data older than 2003, as highlighted in Table 2. Using data from different periods may also lead to additional uncertainty in the results, which is not captured here. Notwithstanding, data from simulations on future forest cover and productivity can be used with the CamBEE framework to estimate the PFRs for the future. This could be particularly needed to anticipate the changes in PFR potential following, e.g., exposure to a warmer climate or mitigation strategies applied in the forestry sector (e.g., shift from less drought-tolerant species to more tolerant ones). Also, the framework does not consider dead or damaged trees as a component of the residual stream (excluded at step 1, where NL is removed from the GAI). This can be seen as underestimating the available theoretical potential; However, the NL are bound to vary due to a plethora of factors such as storms, insects, changing climate, wildfires, among other things [78,79], may be of relatively poor quality, and are seen as a rather unreliable stream for bioeconomy planning, hence its exclusion.

Another limitation related to the value of BEFs, which is contingent on several factors out of which climatic regime of the area and soil attributes are region-specific. BEF are factors widely used to estimate carbon stocks

in forests, allowing to estimate the total aboveground biomass generated by a given class of tree (broad leaves, conifer), knowing the minimum diameter at breast height. Most practitioners rely, as in this study, on the estimates provided by the IPCC [42]. However, the IPCC provides these BEF values as coarse aggregated figures for wide biomes (e.g., temperate). In this way, the use of this factor can be seen as a limitation. Nevertheless, the BEF values are provided as ranges in the IPCC, so it is expected that any spatial variation coming from regional attributes are captured within these ranges.

In terms of energy, 8.4 Million  $\text{Mg}_{\text{dry matter}} \text{ year}^{-1}$  directly translates to ca. 161.2 PJ  $\text{ year}^{-1}$  (considering a LHV of 19.19 GJ  $\text{ Mg}^{-1}$ ). This represents about 2.5 % of France's 2017 energy consumption [74]. The total available potential of PFRs in this assessment includes both private and public forests, with a substantial quantity of these residues (about 74%) lying with private owners. In a survey study involving 800 forest owners across Sweden, Germany, and Portugal, Blennow et al. [80] suggest that private forest owners in Europe may not be willing to contribute to mobilizing the available stemwood (not PFR) for different bioeconomic purposes, which in turns involve no residues generation. However, Stjepan et al. [81] reported that forest owners in South-Eastern Europe are more willing to manage their forests in mobilizing woody biomass for bioeconomic purposes. This highlights the critical importance of these private forest owners as stakeholders to mobilize towards sustainable bioeconomy strategies.

## 6. Conclusions

The essential contributions of the present study are summarized as:

- A generic, transparent and stepwise methodology for spatial quantification of PFRs at the pixel level incorporating associated uncertainties was developed. The applicability of the proposed methodology was tested and demonstrated for the case of Metropolitan France. The results indicated not only that the framework is easy to use, but also that about 8.4 Million  $\text{Mg}_{\text{dry matter}} \text{ year}^{-1}$  of PFRs, the equivalent of 161 PJ  $\text{ year}^{-1}$ , are theoretically available for the bioeconomy in France.
- The uncertainty quantification of PFRs revealed that the available potential of PFRs ranged from about 4.4 Million  $\text{Mg}_{\text{dry matter}} \text{ year}^{-1}$  to about 13.9 Million  $\text{Mg}_{\text{dry matter}} \text{ year}^{-1}$ . This large range highlighted the importance of quantifying uncertainties.
- A clear and transparent procedure to decide the spatial resolution was presented. From this, it is concluded that processing data at very high spatial resolution (< 5-meter) might not necessarily yield better results; instead, it may unnecessarily increase the computational budget without adding any extra value. Here, a resolution of 10-meter was found optimal.

## Acknowledgments

This work was carried out within the framework of the research project Cambioscop (<https://cambioscop.cnrs.fr>), partly financed by the French National Research Agency, Programme Investissement d'Avenir (ANR-17-MGPA-0006) and Region Occitanie (18015981). The authors gratefully acknowledge Dr. Antoine Collin of IGN for insightful discussions, advices, and the access to BD Forêt version 2 data and to Dr. Laurent Polidori and Dr. Jordi Inglada of CESBIO for sharing the land cover data of Metropolitan France. The authors further acknowledge Miriam Buitrago of ADEME for guidance on the ALDO tool. Finally, sincere thanks to Natascha Raue for her diligent proofreading of this paper.

## References:

- [1] IPCC. Summary for Policymakers. In: Global Warming of 1.5°C. An IPCC Special Report on the impacts of global warming of 1.5°C above pre-industrial levels and related global greenhouse gas emission pathways, in the context of strengthening the global response to. In: Masson-Delmotte, V., P. Zhai, H.-O. Pörtner, D. Roberts, J. Skea, P.R. Shukla, A. Pirani, W. Moufouma-Okia, C. Péan, R. Pidcock, S. Connors, J.B.R. Matthews, Y. Chen, X. Zhou, M.I. Gomis, E. Lonnoy, T. Maycock, M. Tignor and TW (eds. ., editor., Oxford, UK: World Meteorological Organization, Geneva, Switzerland, 32 pp.; 2018.
- [2] Le Quéré C, Moriarty R, Andrew RM, Peters GP, Ciais P, Friedlingstein P, et al. Global carbon budget 2014. *Earth Syst Sci Data* 2015;7:47–85. <https://doi.org/10.5194/essd-7-47-2015>.
- [3] UN. Paris Agreement. 2015.
- [4] Hamelin L, Borzeczka M, Kozak M, Pudelko R. A spatial approach to bioeconomy: Quantifying the residual biomass potential in the EU-27. *Renew Sustain Energy Rev* 2019;100:127–42. <https://doi.org/10.1016/j.rser.2018.10.017>.
- [5] Teigiserova DA, Hamelin L, Thomsen M. Review of high-value food waste and food residues biorefineries with focus on unavoidable wastes from processing. *Resour Conserv Recycl* 2019;149:413–26. <https://doi.org/10.1016/j.resconrec.2019.05.003>.
- [6] Tonini D, Hamelin L, Astrup TF. Environmental implications of the use of agro-industrial residues for biorefineries: application of a deterministic model for indirect land-use changes. *GCB Bioenergy* 2016;8:690–706. <https://doi.org/10.1111/gcbb.12290>.
- [7] Daiooglou V, Stehfest E, Wicke B, Faaij A, van Vuuren DP. Projections of the availability and cost of residues from agriculture and

- forestry. *GCB Bioenergy* 2016;8:456–70. <https://doi.org/10.1111/gcbb.12285>.
- [8] Ruiz P, Sgobbi A, Nijs W, Thiel C, Dalla Longa F, Kober T, et al. The JRC-EU-TIMES model. Bioenergy potentials for EU and neighbouring countries. European Commission Joint Research Centre; 2015. <https://doi.org/10.2790/39014>.
- [9] Walmsley JD, Godbold DL. Stump harvesting for bioenergy - A review of the environmental impacts. *Forestry* 2010;83:17–38. <https://doi.org/10.1093/forestry/cpp028>.
- [10] Kaarakka L, Vaittinen J, Marjanen M, Hellsten S, Kukkola M, Saarsalmi A, et al. Stump harvesting in *Picea abies* stands: Soil surface disturbance and biomass distribution of the harvested stumps and roots. *For Ecol Manage* 2018;425:27–34. <https://doi.org/10.1016/j.foreco.2018.05.032>.
- [11] Persson T, Egnell G. Stump harvesting for bioenergy: A review of climatic and environmental impacts in northern Europe and America. *WIREs Energy Environ* 2018;7:e307. <https://doi.org/10.1002/wene.307>.
- [12] Thivolle-Cazat A, Le Net É. La mobilisation de la ressource forestière aujourd'hui et demain. *Rev For Française* 2014;Fr.], ISSN 0035. <https://doi.org/10.4267/2042/56558>.
- [13] Barrette J, Paré D, Manka F, Guindon L, Bernier P, Titus B. Forecasting the spatial distribution of logging residues across the Canadian managed forest. *Can J For Res* 2018;48:1470–81. <https://doi.org/10.1139/cjfr-2018-0080>.
- [14] Návár J. Measurement and assessment methods of forest aboveground biomass: a literature review and the challenges ahead. In: Momba M, Bux F, editors. *Biomass, Sciyo: Rijeka, Croatia*; 2010, p. 27–64.
- [15] FAO. *Global Forest Resources Assessments | Food and Agriculture Organization of the United Nations* 2020. <http://www.fao.org/forest-resources-assessment/en/> (accessed August 20, 2020).
- [16] IGN. *Les données brutes - INVENTAIRE FORESTIER* 2020. <https://inventaire-forestier.ign.fr/spip.php?rubrique159> (accessed August 20, 2020).
- [17] Gschwantner T, Alberdi I, Balázs A, Bauwens S, Bender S, Borota D, et al. Harmonisation of stem volume estimates in European National Forest Inventories. *Ann For Sci* 2019;76:24. <https://doi.org/10.1007/s13595-019-0800-8>.
- [18] Tomppo E, Gschwantner T, Lawrence M, McRoberts RE. *National Forest Inventories*. Dordrecht: Springer Netherlands; 2010. <https://doi.org/10.1007/978-90-481-3233-1>.
- [19] Vidal C, Alberdi I, Redmond J, Vestman M, Lanz A, Schadauer K. The role of European National Forest Inventories for international forestry reporting. *Ann For Sci* 2016;73:793–806. <https://doi.org/10.1007/s13595-016-0545-6>.
- [20] Gschwantner T, Lanz A, Vidal C, Bosela M, Di Cosmo L, Fridman J, et al. Comparison of methods used in European National Forest Inventories for the estimation of volume increment: towards harmonisation. *Ann For Sci* 2016;73:807–21. <https://doi.org/10.1007/s13595-016-0554-5>.
- [21] COST. *COST Action E43 Harmonisation of national Inventories in Europe : Techniques for Common Reporting*. 2008.
- [22] Zhang J, Atkinson P, Goodchild MF. *Scale in Spatial Information and Analysis*. 1st Editio. Boca Raton: CRC Press; 2014. <https://doi.org/10.1201/b16751>.
- [23] López-Rodríguez F, Atanet CP, Blázquez FC, Celma AR. Spatial assessment of the bioenergy potential of forest residues in the western province of Spain, Caceres. *Biomass and Bioenergy* 2009;33:1358–66. <https://doi.org/10.1016/j.biombioe.2009.05.026>.
- [24] Vasco H, Costa M. Quantification and use of forest biomass residues in Maputo province, Mozambique. *Biomass and Bioenergy* 2009;33:1221–8. <https://doi.org/10.1016/j.biombioe.2009.05.008>.
- [25] Viana H, Cohen WB, Lopes D, Aranha J. Assessment of forest biomass for use as energy. GIS-based analysis of geographical availability and locations of wood-fired power plants in Portugal. *Appl Energy* 2010;87:2551–60. <https://doi.org/10.1016/j.apenergy.2010.02.007>.
- [26] Wells LA, Chung W, Anderson NM, Hogland JS. Spatial and temporal quantification of forest residue volumes and delivered costs. *Can J For Res* 2016;46:832–43. <https://doi.org/10.1139/cjfr-2015-0451>.
- [27] Wells LA. *Spatial Distribution and Quantification of Forest Treatment Residues for Bioenergy Production*. University of Montana, 2013.
- [28] Guindon L, Bernier PY, Beaudoin A, Pouliot D, Villemaire P, Hall RJ, et al. Annual mapping of large forest disturbances across Canada's forests using 250 m MODIS imagery from 2000 to 2011. *Can J For Res* 2014;44:1545–54.
- [29] Guindon L, Villemaire P, St-Amant R, Bernier PY, Beaudoin A, Caron F, et al. Canada Landsat Disturbance (CanLaD): a Canada-wide Landsat-based 30-m resolution product of fire and harvest detection and attribution since 1984 2017. <https://doi.org/10.23687/add1346b-f632-4eb9-a83d-a662b38655ad>.
- [30] Greggio N, Balugani E, Carlini C, Contin A, Labartino N, Porcelli R, et al. Theoretical and unused potential for residual biomasses in the emilia Romagna Region (Italy) through a revised and portable framework for their categorization. *Renew Sustain Energy Rev* 2019;112:590–606. <https://doi.org/10.1016/j.rser.2019.06.019>.
- [31] Vis MW, van den Berg D, Al. E. *Best Practices and Methods Handbook* 2010;D 5.3:1–220.
- [32] Domingo D, Montealegre AL, Lamelas MT, García-Martín A, de la Riva J, Rodríguez F, et al. Quantifying forest residual biomass in *Pinus halepensis* Miller stands using Airborne Laser Scanning data. *GIScience Remote Sens* 2019;0:1–23. <https://doi.org/10.1080/15481603.2019.1641653>.
- [33] Batidzirai B, Smeets EMW, Faaiz APC. Harmonising bioenergy resource potentials - Methodological lessons from review of state of the art bioenergy potential assessments. *Renew Sustain Energy Rev* 2012;16:6598–630. <https://doi.org/10.1016/j.rser.2012.09.002>.
- [34] European Commission. *A new EU Forest Strategy: For forests and the forest-based sector*. Commun from Comm to Eur Parliam Councils, Eur Econ Soc Comm Comm Reg Brussels 2013.
- [35] List of Annex I Countries - OECD n.d. <http://www.oecd.org/env/cc/listofannexicountries.htm> (accessed September 23, 2019).
- [36] *Inventory Review Reports 2019 | UNFCCC* n.d. <https://unfccc.int/process-and-meetings/transparency-and-reporting/reporting-and-review-under-the-convention/greenhouse-gas-inventories-annex-i-parties/inventory-review-reports/inventory-review-reports-2019> (accessed September 23, 2019).
- [37] Kindermann GE, McCallum I, Fritz S, Obersteiner M. A global forest growing stock, biomass and carbon map based on FAO statistics. *Silva Fenn* 2008;42:387–96.
- [38] Rengarajan R, Sampath A, Storey J, Choate M. Validation of geometric accuracy of global land survey (GLS) 2000 data. *Photogramm Eng Remote Sensing* 2015;81:131–41. <https://doi.org/10.14358/PERS.81.2.131>.
- [39] ESA. *Download CCI LC Products | ESA CCI Land cover website* 2015. <https://www.esa-landcover-cci.org/?q=node/164> (accessed August 20, 2020).
- [40] Jun C, Ban Y, Li S. Open access to Earth land-cover map. *Nature* 2014;514:434. <https://doi.org/10.1038/514434c>.
- [41] *EEA. Corine land cover 2000. Technical guidelines*. 2002.
- [42] *IPCC. Good Practice Guidance for Land Use, Land-Use Change and Forestry*. 2003.
- [43] Reyes G, Brown S, Chapman J, Lugo AE. *Wood Densities of Tropical Tree Species*. 1992. <https://doi.org/10.2737/SO-GTR-88>.
- [44] Schroeder P, Brown S, Mo J, Birdsey R, Cieszewski C. *Biomass Estimation for Temperate Broadleaf Forests of the United States*

- Using Inventory Data. *For Sci* 1997;43:424–34.
- [45] Sanquetta CR, Corte APD, da Silva F. Biomass expansion factor and root-to-shoot ratio for Pinus in Brazil. *Carbon Balance Manag* 2011;6:6. <https://doi.org/10.1186/1750-0680-6-6>.
- [46] Schoene D, Killmann W, Von Lupke H, LoycheWilkie M. Definitional issues related to reducing emission from deforestation in developing countries. *FAO Rep* 2007:1–26.
- [47] FAO. *Forest Resources of Europe, CIS, North America, Australia, Japan and New Zealand (TBFRA-2000)*. vol. 81. 2000.
- [48] Qin L, Liu Q, Zhang M, Saeed S. Effect of measurement errors on the estimation of tree biomass. *Can J For Res* 2019;49:1371–8. <https://doi.org/10.1139/cjfr-2019-0034>.
- [49] Westfall JA, McRoberts RE. An assessment of uncertainty in volume estimates for stands reconstructed from tree stump information. *Forestry* 2017;90:404–12. <https://doi.org/10.1093/forestry/cpw064>.
- [50] McRoberts RE, Westfall JA. Propagating uncertainty through individual tree volume model predictions to large-area volume estimates. *Ann For Sci* 2016;73:625–33. <https://doi.org/10.1007/s13595-015-0473-x>.
- [51] Kuliešis A, Tomter SM, Vidal C, Lanz A. Estimates of stem wood increments in forest resources: comparison of different approaches in forest inventory: consequences for international reporting: case study of European forests. *Ann For Sci* 2016;73:857–69. <https://doi.org/10.1007/s13595-016-0559-0>.
- [52] Schmidt FL, Hunter JE. Theory Testing and Measurement Error. *Intelligence* 1999;27:183–98. [https://doi.org/10.1016/S0160-2896\(99\)00024-0](https://doi.org/10.1016/S0160-2896(99)00024-0).
- [53] Joint Committee For Guides In. *Evaluation of measurement data — Guide to the expression of uncertainty in measurement*. Int Organ Stand Geneva ISBN 2008;50:134. <https://doi.org/10.1373/clinchem.2003.030528>.
- [54] Farrance I, Frenkel R. Uncertainty of measurement: A review of the rules for calculating Uncertainty components through functional relationships. *Clin Biochem Rev* 2012;33:49–75.
- [55] Weidema BP, Wesnæs MS. Data quality management for life cycle inventories—an example of using data quality indicators. *J Clean Prod* 1996;4:167–74. [https://doi.org/10.1016/S0959-6526\(96\)00043-1](https://doi.org/10.1016/S0959-6526(96)00043-1).
- [56] Eurostat. *Statistical regions in the European Union and partner countries. NUTS and statistical regions 2021*. 2020. <https://doi.org/10.2785/850262>.
- [57] European Commission. *A sustainable Bioeconomy for Europe: strengthening the connection between economy, society and the environment*. 2018. <https://doi.org/10.2777/478385>.
- [58] Over 40% of the EU covered with forests - Product - Eurostat n.d. <https://ec.europa.eu/eurostat/web/products-eurostat-news/-/EDN-20180321-1> (accessed December 13, 2019).
- [59] IGN. *Le mémento*. 2017. [https://inventaire-forestier.ign.fr/IMG/pdf/memento\\_2017.pdf](https://inventaire-forestier.ign.fr/IMG/pdf/memento_2017.pdf)
- [60] Schmithusen F, Hirsch F. Private forest ownership in Europe. *Geneva Timber For Study Pap* 26, UNECE 2010:1–120.
- [61] Forests in France - GEVES n.d. <https://www.geves.fr/variety-seed-expertise/forest/forestry-in-france/> (accessed December 13, 2019).
- [62] IGN. *BD Forêt® Version 2.0 - Descriptif de contenu*. 2018. [https://geoservices.ign.fr/ressources\\_documentaires/Espace\\_documentaire/BASES\\_VECTORIELLES/BDFORET/DL\\_BDForet\\_2-0.pdf](https://geoservices.ign.fr/ressources_documentaires/Espace_documentaire/BASES_VECTORIELLES/BDFORET/DL_BDForet_2-0.pdf)
- [63] ADEME. *L'outil aldo, pour une première estimation de la séquestration carbone dans les sols et la biomasse* 2019. <https://www.territoires-climat.ademe.fr/actualite/loutil-aldo-pour-une-premiere-estimation-de-la-sequestration-carbone-dans-les-sols-et-la-biomasse> (accessed August 20, 2020).
- [64] GDAM. *GADM data 2018*. <https://gadm.org/data.html> (accessed August 20, 2020).
- [65] *Contours of EPCI 2015 - data.gouv.fr n.d.* <https://www.data.gouv.fr/fr/datasets/contours-des-epci-2015/> (accessed October 11, 2019).
- [66] *Public forests (public distribution) - data.gouv.fr n.d.* <https://www.data.gouv.fr/fr/datasets/forets-publiques-diffusion-publique/> (accessed October 14, 2019).
- [67] IPCC. Chapter 4: Forest Land. 2019 Refinement to 2006 IPCC Guidel. *Natl. Greenh. Gas Invent.* eds. Raul Abad Vinas, Val. Avitabile, Luca Birigazzi, Simone Ross. Danae M. A. Rozendaal, Louis Verchot., 2019.
- [68] Colin A, Simon M, Roos E, Schwarz Y. *Contribution de l'IGN à l'établissement des bilans carbone des forêts des territoires (PCAET) 2019*.
- [69] ESRI. *Data classification methods—ArcGIS Pro | Documentation 2020*. <https://pro.arcgis.com/en/pro-app/help/mapping/layer-properties/data-classification-methods.htm> (accessed August 20, 2020).
- [70] Hansen MC, Potapov P V, Moore R, Hancher M, Turubanova SA, Tyukavina A, et al. High-Resolution Global Maps of 21st-Century Forest Cover Change. *Science (80- )* 2013;342:850 LP – 853. <https://doi.org/10.1126/science.1244693>.
- [71] Inglada J, Vincent A, Arias M, Tardy B, Morin D, Rodes I. Operational High Resolution Land Cover Map Production at the Country Scale Using Satellite Image Time Series. *Remote Sens* 2017;9:95. <https://doi.org/10.3390/rs9010095>.
- [72] EOS. *Satellite Data: What Spatial Resolution Is Enough for You?* 2020. <https://eos.com/blog/satellite-data-what-spatial-resolution-is-enough-for-you/> (accessed August 20, 2020).
- [73] Martinkus N, Latta G, Morgan T, Wolcott M. A comparison of methodologies for estimating delivered forest residue volume and cost to a wood-based biorefinery. *Biomass and Bioenergy* 2017;106:83–94. <https://doi.org/10.1016/j.biombioe.2017.08.023>.
- [74] IEA. *Data tables – Data & Statistics 2020*. <https://www.iea.org/data-and-statistics/data-tables?country=FRANCE&energy=Balances&year=2017> (accessed August 20, 2020).
- [75] Brassard P, Godbout S, Hamelin L. Framework for consequential life cycle assessment of pyrolysis biorefineries : A case study for the conversion of primary forestry residues. *EarthArXiv* 2020. <https://doi.org/10.31223/osf.io/3qfc4>.
- [76] Colin A, Thivolle A. *Disponibilités Forestières Pour l'Energie Et Les Matériaux à l'Horizon 2035*. Ademe 2016:1–91.
- [77] IGN. *Large ecological regions (GRECO) | geo.data.gouv.fr 2015*. <https://geo.data.gouv.fr/fr/datasets/6c8a6dc109c93f05365752e494ba4643dce882fa> (accessed August 20, 2020).
- [78] Curtis PG, Slay CM, Harris NL, Tyukavina A, Hansen MC. Classifying drivers of global forest loss. *Science (80- )* 2018;361:1108–11. <https://doi.org/10.1126/science.aau3445>.
- [79] Seidl R, Thom D, Kautz M, Martin-Benito D, Peltoniemi M, Vacchiano G, et al. Forest disturbances under climate change. *Nat Clim Chang* 2017;7:395–402. <https://doi.org/10.1038/nclimate3303>.
- [80] Blennow K, Persson E, Lindner M, Faia SP, Hanewinkel M. Forest owner motivations and attitudes towards supplying biomass for energy in Europe. *Biomass and Bioenergy* 2014;67:223–30. <https://doi.org/10.1016/j.biombioe.2014.05.002>.
- [81] Stjepan P, Mersudin A, Dženan B, Nenad P, Makedonka S, Dane M, et al. Private forest owners' willingness to supply woody biomass in selected South-Eastern European countries. *Biomass and Bioenergy* 2015;81:144–53. <https://doi.org/10.1016/j.biombioe.2015.06.011>.